POLSKA AKADEMIA NAUK
INSTYTUT MASZYN PRZEPŁYWOWYCH

PRACE INSTYTUTU MASZYN PRZEPŁYWOWYCH

TRANSACTIONS
OF THE INSTITUTE OF FLUID-FLOW MACHINERY

70-72

WARSZAWA–POZNAŃ 1976

PAŃSTWOWE WYDAWNICTWO NAUKOWE

PRACE INSTYTUTU MASZYN PRZEPŁYWOWYCH

poświęcone są publikacjom naukowym z zakresu teorii i badań doświadczalnych w dziedzinie mechaniki i termodynamiki przepływów, ze szczególnym uwzględnieniem problematyki maszyn przepływowych

*

THE TRANSACTIONS OF THE INSTITUTE OF FLUID-FLOW MACHINERY

exist for the publication of theoretical and experimental investigations of all aspects of the mechanics and thermodynamics of fluid-flow with special reference to fluid-flow machinery

REDAKCJA – EDITORIAL OFFICE
Instytut Maszvn Przepływowych PAN
ul. Gen. Józefa Fiszera 14, 80-952 Gdańsk, skr. pocztowa 621, tel. 41-12-71

PAŃSTWOWE WYDAWNICTWO NAUKOWE – ODDZIAŁ W POZNANIU

Wydanie I. Nakład 630+90 egz. Ark. wyd. 63,25 Ark. druk. 49,25 Papier druk. sat. kl. V. 65 g., 70×100. Oddano do składania 4 VII 1975 r. Podpisano do druku w czerwcu 1976 r. Druk ukończono w czerwcu 1976 r. Zam. 528/118. H-16/245.
Cena zł 190,–

DRUKARNIA UNIWERSYTETU IM. ADAMA MICKIEWICZA W POZNANIU

III KONFERENCJA NAUKOWA

na temat

TURBINY PAROWE WIELKIEJ MOCY

Gdańsk, 24 - 27 września 1974 r.

*

IIIrd SCIENTIFIC CONFERENCE

on

STEAM TURBINES OF GREAT OUTPUT

Gdańsk, September 24 - 27, 1974

*

III НАУЧНАЯ КОНФЕРЕНЦИЯ

на тему

ПАРОВЫЕ ТУРБИНЫ БОЛЬШОЙ МОЩНОСТИ

Гданьск, 24 - 27 сентября 1974 г.

PRACE INSTYTUTU MASZYN PRZEPŁYWOWYCH
1976 Zeszyt 70 - 72

PAUL T. WALTERS, MICHAEL J. MOORE

Great Britain*

The Measurement of Circumferential Flow Variations in the Final Stage of L. P. Turbines

1. Introduction

Axisymmetric design methods based on the streamline curvature principle [1, 2] provide a means of considerably improving the aerodynamic performance of large steam turbines. The successful application of these methods, however, relies essentially on detailed and accurate input data relating to elements of the machine such as the effective casing geometry and the distribution of blading losses.

For the region near the casing in the final stage of large L. P. turbines it is particularly difficult to specify these data. The shape of the casing is complicated by bled-steam extraction belts and the highly flared wall is interrupted by axial sections at the moving blade tips to allow for differential expansion. Also a complex flow structure is produced by the interaction between the tip leakage flow from the penultimate stage and the secondary flows in the fixed blade row. To provide the information necessary for improved theoretical modelling of the flow in this region, detailed measurements have been made in L. P. turbine cylinders.

Access to this part of the machine was achieved by a circumferentially traversing probe that enabled total pressure surverys to be made over a region extending inwards from the casing wall in the exit plane of the fixed blades. In addition traverses with pitot-static-yawmeter probes gave the complementary radial distributions of static pressure and flow angle. Results are presented for the two 500 MW turbines in which measurements have been completed; they are referred to as turbines A and B in this paper.

2. The instrumentation of L.P. turbines

Access for instrumentation in L. P. turbines was achieved by means of radial guide tubes which extended from the inner casing to the outside of the turbine where they were terminated by gate valves. Probes could then be inserted via the gate valves, traversed in the steam space and removed whilst the turbine was on load without affecting its opera-

* Central Electricity Research Laboratories, Leatherhead, Surrey.

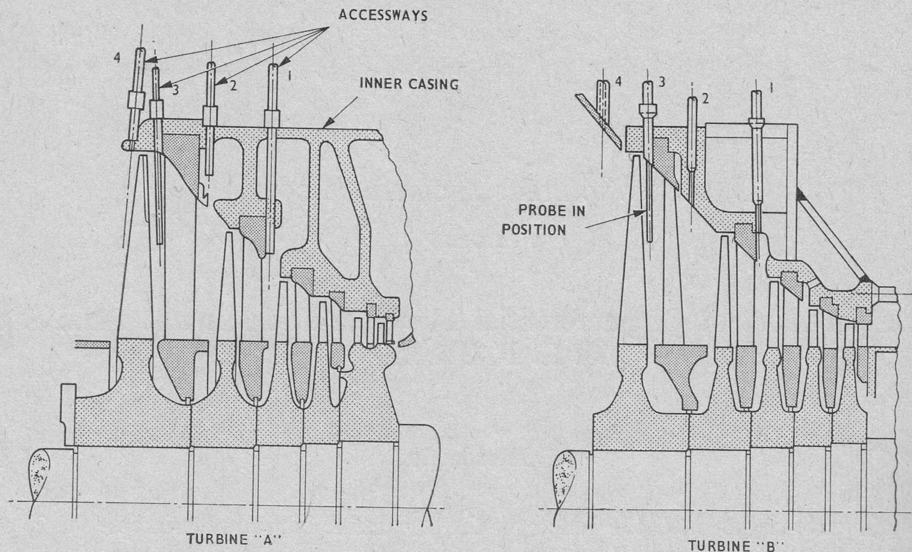

Fig. 1. Details of turbine casings and probe accessways

tion. The diameter of the probe bodies was restricted to one inch (25.4 mm) which is a good compromise between the aerodynamic requirement of a small steam and the rigidity required for extensions of up to one metre in high velocity flows.

The positions of the accessways in the L.P. cylinders of the two turbines discussed in this paper are shown in approximate longitudinal sections in Fig. 1. Generally, ample

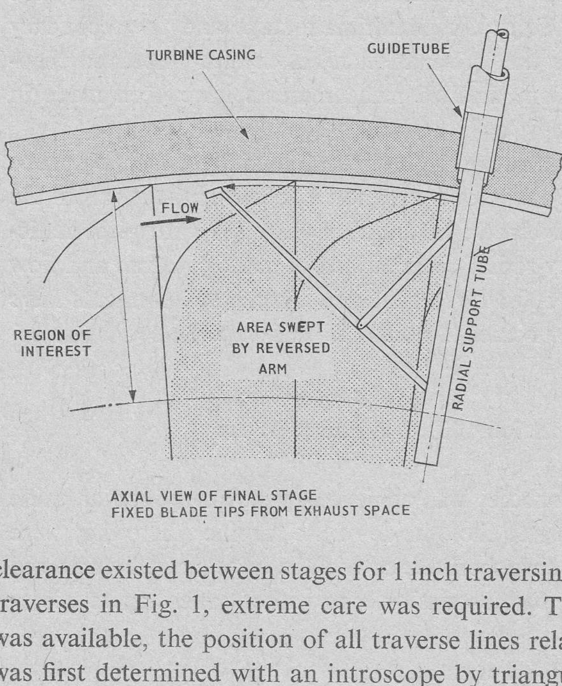

Fig. 2. Principle of circumferential traversing with reversed arm mechanism

clearance existed between stages for 1 inch traversing probes, but in-stage, as in the number 3 traverses in Fig. 1, extreme care was required. To ensure that a safe working clearance was available, the position of all traverse lines relative to the blading in the cold position was first determined with an introscope by triangulation from the known blade pitching.

Then, before traversing was commenced, a dummy probe carrying strain gauges and an accelerometer was carefully extended into the steam space when the machine was on load to determine the deflection and vibration of the probes under the static and dynamic loading imposed by the flow. The overall structure of the flow may be defined from the general axisymmetry of the cylinder by radial traversing alone. Instrumentation is subsequently described for measuring the radial distributions of pressure velocity and flow angle. However, to investigate the complex flow in the tip region of the final stage, a circumferentially traversing probe was designed which is shown in principle in Fig. 2. The tip of a reversed arm is extended laterally from a radial support tube by a simple mechanism and describes a virtually circumferential locus. A region extending almost to the casing wall can therefore be surveyed by circumferential traverses at a series of radial intervals.

3. Instruments for flow measurements in L.P. turbines

3.1. Radial traversing probes

Most of the radial traverse data were obtained with the probe shown in Fig. 3a which consists of a disc static-yawmeter combined with a hooded total pressure or "Kiel" probe. For this application the disc has the advantage that alignment with the flow is achieved by nulling between static pressures, in contrast with the familiar "arrowhead" yawmeter which depends largely on the velocity head. The correct flow angle is therefore indicated by the disc even in a velocity gradient such as a fixed blade wake. The disc is also inherently insensitive to the pitch angle variations that occur over a radial traverse.

The disc profile, an ellipse with a thickness of 16%, was selected following some development as the best compromise between sensitivity to yaw misalignment and accuracy of the indicated static pressure.

The Kiel probe design was that of Gracey, Coletti and Russel [3] which will register total pressures with an error of less than 1% for incidences of up to 56° to the probe axis in flows of Mach number less than 1.1. The assembly of the combined probe ensured negligible aerodynamic interference between its elements and steam according to the data of Schulz, Ashby and Erwin [4].

The pitch angle component of the flow direction was measured with the instrument shown in Fig. 3b. A "Conrad" probe was set in the predetermined yaw plane and aligned with the flow by the familiar nulling method. The rotation of the probe head was effected by a push rod driven by a micrometer screw at the remote end of the instrument.

Finally the total temperature probe shown in Fig. 3c was constructed as superheated conditions are sometimes encountered at entry to the penultimate stage at part load and in the tip leakage jet. The probe is a conventional, high recovery factor design and was used for an exploratory traverse wherever superheated steam conditions were suspected.

The probes were calibrated in the C.E.R.L. wet steam tunnel, a facility which is described by Moore, Walters, Crane and Davidson [5]. The performance of the Kiel probe, in fact, slightly exceeded the claims of [3] but the disc required calibrating against a

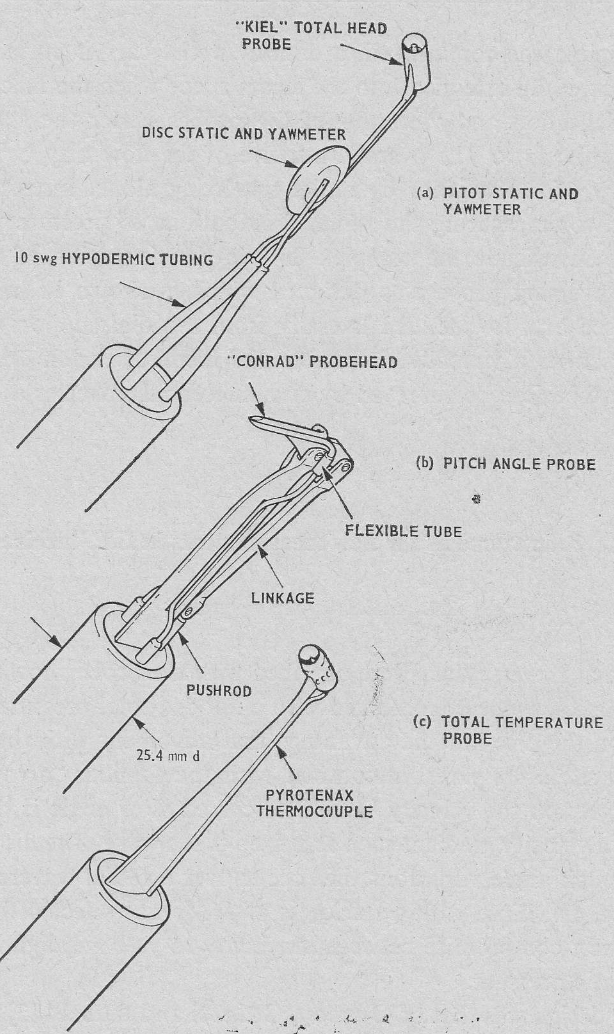

Fig. 3. Radial traversing probes

standard and showed in the indicated static pressure a slight deficit, which was found to be a function of Mach number only. The characteristics of the pitch probe varied only slightly over a large range of Mach number and a single direct calibration of pitch angle as a function of micrometer setting was adopted with sufficient accuracy.

3.2. The circumferential traversing probe

The investigation of the tip region of the final stage took the form of total pressure surveys in planes at exit from the fixed and moving blades, an extension, in fact, of the frequently reported model cascade experiments e.g. Came [6], Turner [7] and Rohlik *et al.* [8], to the real turbine situation. From Fig. 2 it can be appreciated that, in traversing a fixed blade pitch, the reversed arm rotates through about 35°. Total pressure surveys with a Kiel probe [3] fixed to the arm and aligned with the flow at mid traverse would therefore be very accurate over the entire area.

To extend this region to the casing wall, a mechanism was designed to produce a traversing locus that closely followed the casing circumference. From Fig. 2 it can be appreciated that this requires a pivot on the traverse arm that moves radially outwards at a rate related to the lateral extension of the arm. This motion was achieved with the mechanism shown in Fig. 4, where the traversing arm is incorporated into a modified Scott-Russel linkage (see Green [9] p. 221). The required traversing locus is obtained by actuating the mechanism by concentric push rods driven by opposing lead screws of differential pitch. Link dimensions and lead screw pitches producing a traverse line that

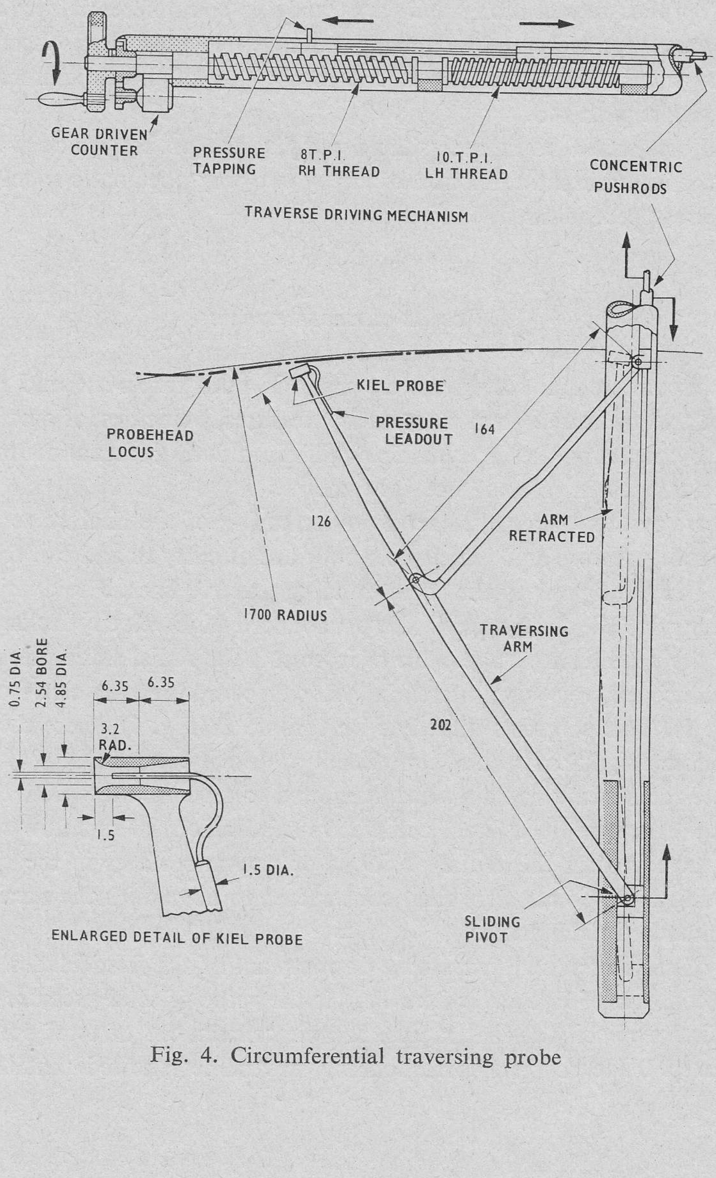

Fig. 4. Circumferential traversing probe

followed a specific turbine casing circumference to within less than 2 mm over 1.5 fixed blade pitches were determined by a few graphical trials. This mechanism was also incorporated into a 25.4 mm dia. tube and proved to be both robust and free from any significant 'backlash'. A numerical counter driven from the leadscrew shaft was calibrated to give the length of arc traversed by the arm.

Traverses were made in the undistorted flow well upstream of the support tube as shown in Fig. 2. The Kiel probe head was set on the arm to align at mid traverse with the flow direction measured by the radial traversing probes. The calculation of this compound angle and the change in incidence during a circumferential traverse is given in Appendix 1.

Much of the operational procedure was common to all probes. For protection during the insertion and removal from the turbine, probeheads were retracted into the support tubes. "Radial" probes retract along their axes and the circumferential probe as shown in Fig. 4. Pressures were measured by remote variable reluctance transducers connected to the probes by small diameter tubing which, in the case of the circumferential probe, was ducted through a push-rod.

Operation in wet steam flows necessitated purging the probes which was easily accomplished by the intermittent admission of air by two-way pneumatic spool valves connected into the pressure lead-outs.

4. Results of measurements

Radial and circumferential traverses were made in both turbine *A* and *B* at or near full load. From the measured total and static pressures, velocities of wet steam flows were calculated by assuming thermodynamic equilibrium during stagnation and a mixture density based on the design value of wetness fraction.

Radial traverse results obtained near the outer casing of the final stage are given in Figs. 5 and 6. Static pressure and velocity distributions at entry to and exit from the fixed blade are related in the figures to the corresponding traverse lines. The dominant feature of the flow at entry to the final stage is the pronounced high velocity leakage flow from the rotor tip of the penultimate stage. Also of interest is the radial static pressure gradient in turbine *A* induced by the circumferential velocity component at exit from the fixed blades (see Fig. 5). This contrasts directly with turbine *B* (Fig. 6) where the casing wall permits in addition a significant radial component of velocity.

The complete radial traverse data were integrated to give the mass flow through each plane containing a traverse line. Equal cumulative subdivisions of this flow starting from the blade root gave in turn the radial positions of stream surfaces in the cylinder. The streamlines joining these points were then constructed to align with the meridional component of the measured pitch angle.

The results of circumferential traversing downstream of the fixed blades are given in Figs. 7 and 8 as contours of $P_t/P_{t\max}$, where $P_{t\max}$ is the value of total pressure corresponding to the maximum velocity at that radius. Sample calculations of total pressure before and after the fixed blade row on corresponding streamlines showed that the upstream

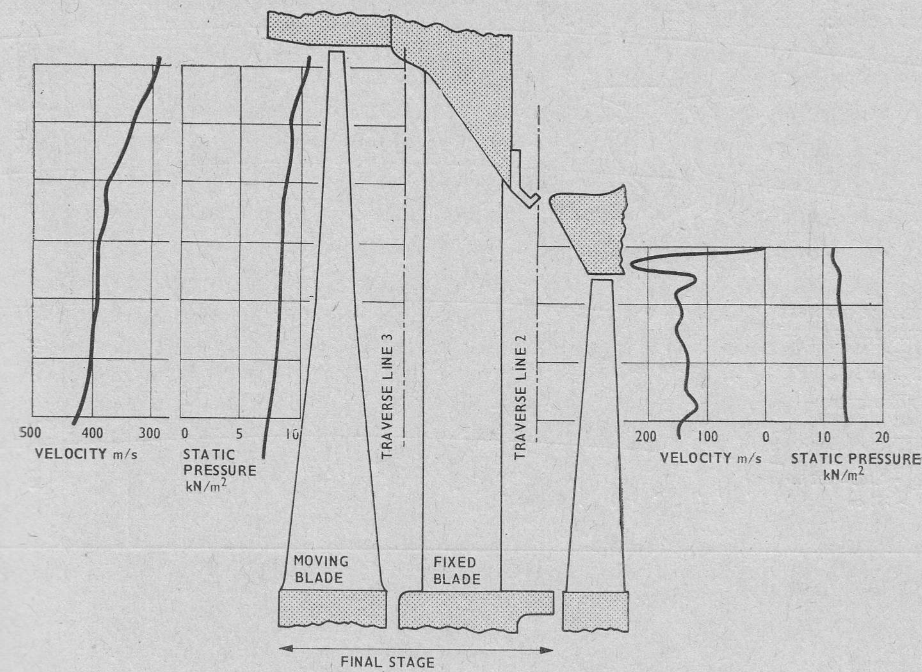

Fig. 5. Radial traverse results turbine *A*

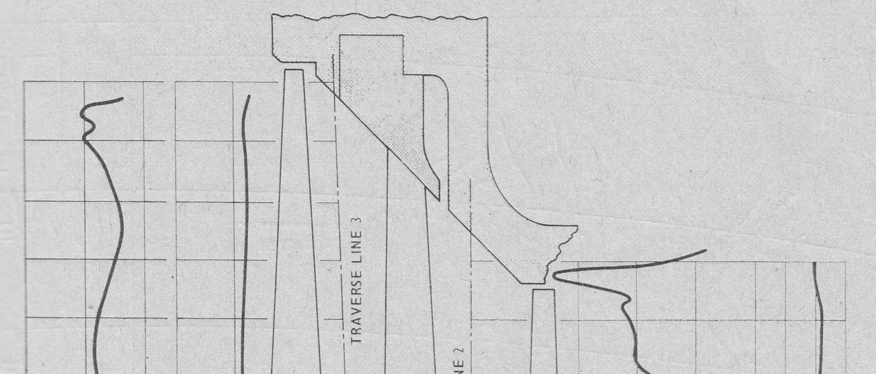

Fig. 6. Radial traverse results turbine *B*

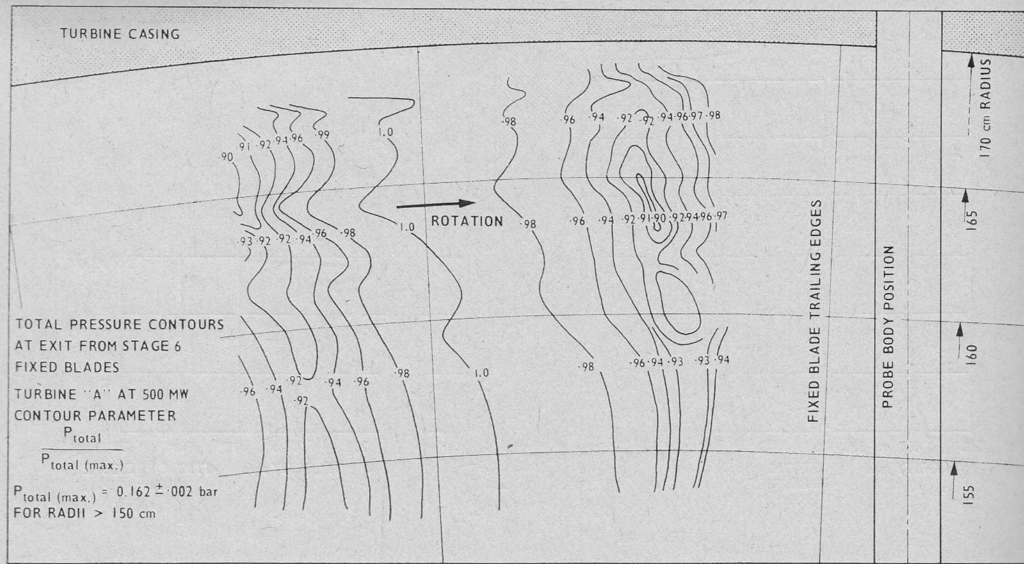

Fig. 7. Turbine *A* total pressure contours

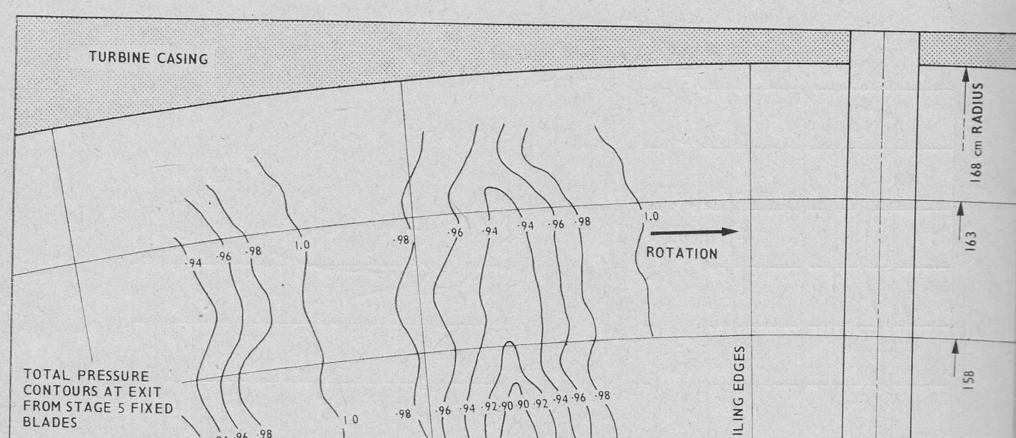

Fig. 8. Turbine *B* total pressure contours

total pressure was in each case also approximately equal to $P_{t\max}$. It is concluded, therefore, that the region of high velocity flow between the wakes has passed through the fixed blades near-isentropically. This appears to be consistent with the contours of total pressure in Figs. 7 and 8, where filling of the blade wakes is evidently incomplete. These contours therefore give not only an impression of the flow structure, but can also provide a detailed distribution of aerodynamic loss as follows.

The flow at exit from the fixed blade tips of both machines is subsonic and is shown by the total pressure contours, Figs. 7 and 8, to contain no strong secondary vortices.

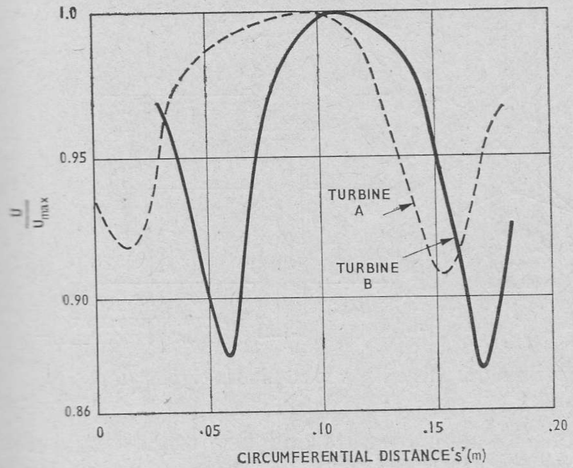

Fig. 9. Circumferential velocity distributions, $R=1.55$ m

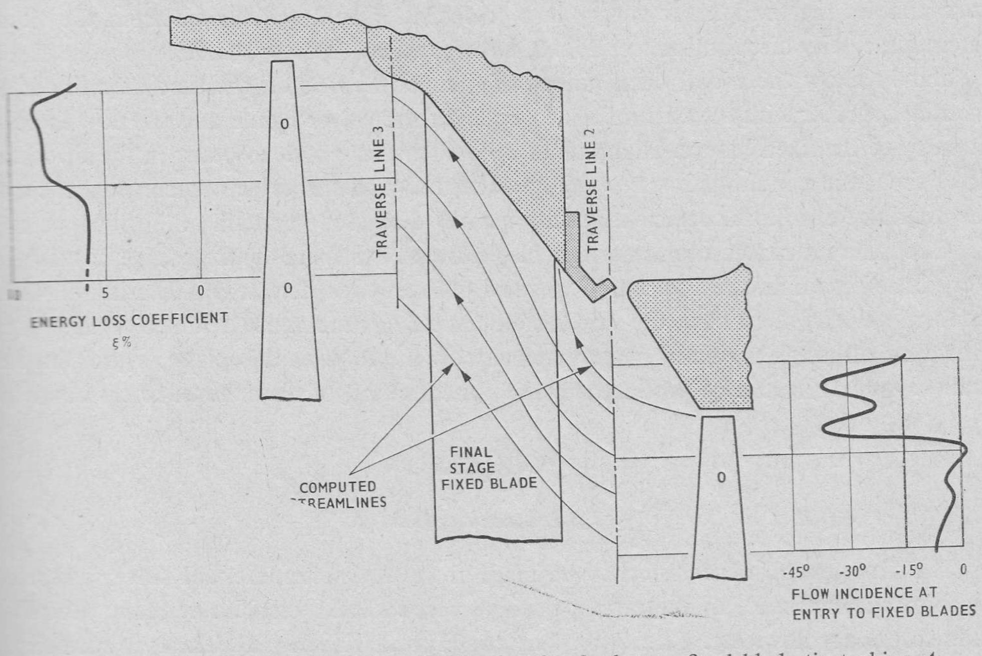

Fig. 10. Incidence at inlet and loss distribution for final stage fixed blade tip turbine *A*

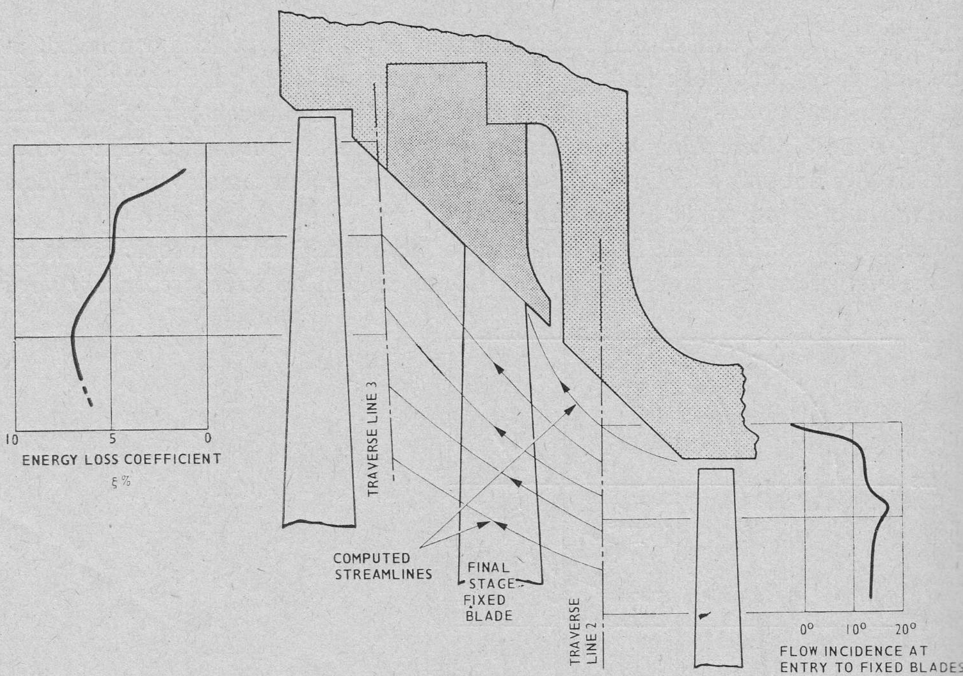

Fig. 11. Inlet incidence and loss distribution. Final stage fixed blades turbine *B*

Significant local circumferential variations in static pressure and flow angle would not therefore occur in this region and sufficient additional data are available from radial traverses for the velocity fields to be calculated from the total pressure surveys. This in turn enables the fixed blade energy loss coefficient ξ to be calculated from the circumferential velocity distribution, see Fig. 9, at any radius, as described in Appendix II. Figs. 10 and 11 show the radial distributions of ξ superimposed on the turbine cylinder geometries, together with the streamlines computed from traverse data and the flow incidence at entry to the fixed blades. High values of incidence are seen to occur in the tip leakage flows from the penultimate stage 1 (Figs. 5 and 6) and the evident correspondence with the distribution of loss coefficient is subsequently discussed in detail.

Circumferential measurements were also made at exit from the final stage of turbine *A*. Very little circumferential variation in total pressure was detected, indicating an almost uniform velocity field over the 1.5% of the total circumference scanned by the probe. However, although no fine structure remains in the flow at this plane, significant large scale asymmetry could be produced by the configuration of the exhaust to the condenser.

5. Discussion

5.1. Secondary flows

The first general observation to be made from the circumferential traverse results is the noticeable absence of the strong passage vortices characteristic of many model cascade secondary flows e.g. Came [6], Turner [7] and Klein [11]. The loss coefficient in turbine B in fact diminishes towards the casing whereas an increase would normally be expected. In this machine, however the geometry of the fixed blade is unusual for a final L.P. stage being both highly twisted and relatively narrow. At the casing wall a short blade profile with very little curvature is presented to the flow at virtually zero incidence, see Fig. 11, which would account for the high local efficiency. Away from the casing the progressive increase in incidence at entry is matched by a corresponding rise in the loss coefficient.

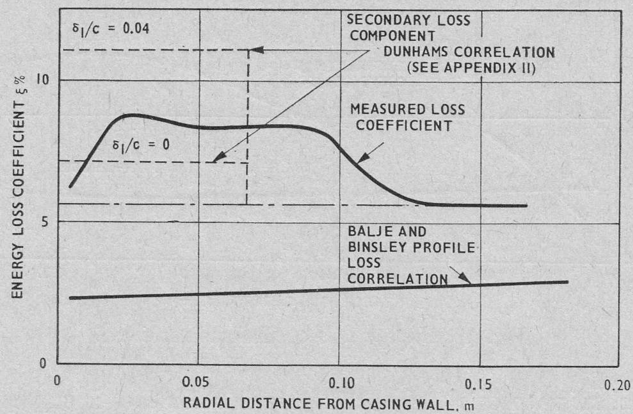

Fig. 12. Energy loss coefficients turbine A

Turbine A on the other hand is more typical of general design practice and does show a local increase in loss coefficient near the casing that could be the result of secondary flows in the fixed blades. At first sight this appears to be confirmed by Dunham's correlation ([10] see Appendix II) as shown in Fig. 12. The theoretical secondary loss coefficient is calculated for the values of inlet wall boundary layer thickness δ_1/C which, according to data assembled by Came [6], cover the range over which secondary loss rises to a maximum. However, the simple concept of the inlet wall boundary layer is difficult to reconcile with the practical situation of the final stage in an L.P. turbine.

The flow structure near the casing at inlet to the fixed blades is extremely complex, consisting of a reattaching high velocity annular leakage jet from the tips of the penultimate stage. The inlet wall "boundary layer" will therefore be highly energised and a value of $\delta_1/C=0$ could give, in effect, an overestimate of the secondary loss coefficient. On this basis the local loss in turbine A appears to be too high to be entirely the result of secondary flows and an alternative source of this loss is suggested below.

5.2. Profile loss

Theoretical values of profile loss calculated by the correlation method of Balje and Binsley [2] are shown compared with the measured values for each turbine in Figs 12 and 13. The predictions underestimate the losses by about 100% even in the region away from the casing where the loss mechanism is not complicated by secondary flows. Some part of this loss may be due to the presence of water on the blade surface and the re-entrainment of this water in the wake region. Kirillov and Yablonik [17] provide some evidence of increases in profile loss as one of the components of the "wetness-losses" in wet steam turbines. Further information is required to confirm this interpretation but it is evident that predictions from simple profile loss correlations can be significantly in error when applied to an L.P. steam turbine.

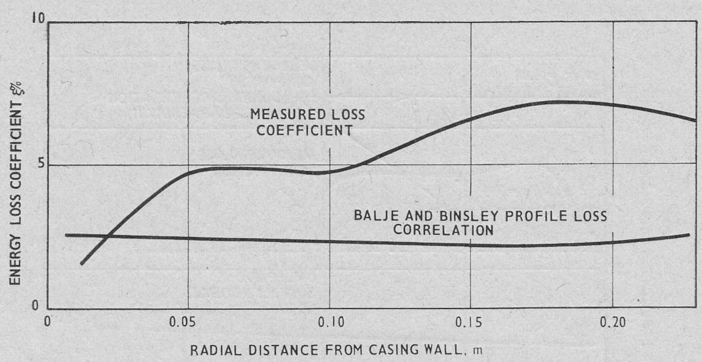

Fig. 13. Energy loss coefficients turbine *B*

A second mechanism possibly producing high profile loss is suggested by the results of Rohlik *et al.* [8]. It was found in annular cascades with similar outlet Mach numbers to L.P. final stage fixed blades, that the radial pressure gradient transferred low momentum fluid from the casing down the trailing edges of the blades. This is particularly pertinent to turbine *A* where the wide wakes, Fig. 9, imply the presence of a separated region on the blade suction surface in which this radial flow could occur. This argument, however could not be applied to turbine *B* where no radial pressure gradient is present. It is apparent, therefore, that improved information is required on blading profile loss in the real L.P. turbine situation.

Returning to the particular phenomenon of the locally high loss region near the casing of turbine *A*, it is shown in Fig. 11 that this may also be interpreted as an exceptional profile loss. The calculated streamlines connect this region with the tip leakage-flow from the preceding stage which enters the fixed blades at high negative incidence. Increased losses would be expected at such adverse incidence and, to support this interpretation of the results, no such high loss region occurs in turbine *B* where inlet flow incidence is small.

5.3. Axisymmetry

The assumption of axisymmetry is pertinent to both the calculation of flows in turbines and to their verification by measurements along radial traverses. Downstream of the fixed blades the assumption of axisymmetry is obviously untenable as shown in Figs. 7, 8 and 9. However, for calculations of continuity of mass flow, integration of circumferential velocity distributions indicates a correction for the displacement thickness of the wakes of only about 5%.

The almost uniform total pressure field observed downstream from the rotor in turbine *A* indicates that wakes virtually fill over the relatively long flow path (50 cm) between the fixed blade trailing edges and the traverse plane. The mixing process in wake transport through blade rows described by Kerrebrock and Mikolajczack [14] having been found in this respect to be a relatively small effect.

Further evidence for generally assuming axisymmetry between stages is provided by radial traverse data. In general it can be shown that several fixed blade wakes cross the radial traverse lines, but no evidence of these wakes is found in the measured radial velocity distributions. Fig. 14 shows the result for the case in question, downstream of the rotor in turbine *A*.

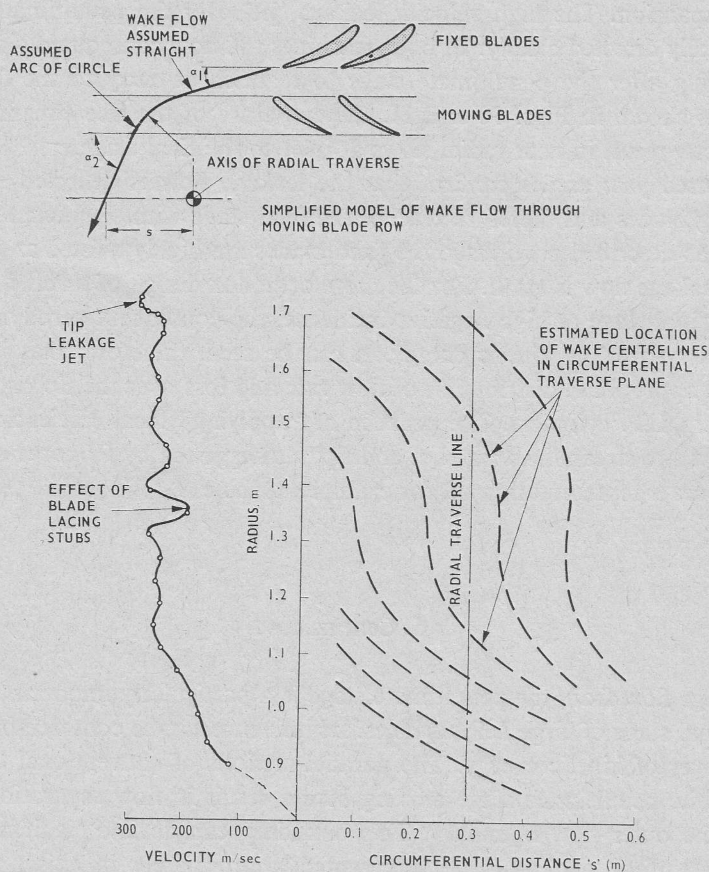

Fig. 14. Position of wakes on radial velocity distribution downstream from final stage turbine *A*

As noted previously, general flow asymmetry may be introduced at this position by the exhaust system which would not be detected over the limited range of circumferential traverses. However this asymmetry will generally have a negligible influence on the flow upstream of the rotor where the flow velocity relative to the moving blades often constitutes a choked condition. The absence of residual wake structure downstream from the rotor indicates flow between stages can be considered to be effectively axisymmetric.

5.4. Tip leakage

The leakage flow from the moving blade tips of the penultimate stage appears to be the dominant factor, in both turbines, in determining the subsequent flow through the tip region of the final stage. The highly flared casings, in common with many large L.P. turbines, incorporate short cylindrical sections at the moving blade tips to accomodate differential expansion. The high velocity leakage 'jet' over the penultimate rotor tips is therefore initially directed axially. In both machines the flow consequently separates from the outer casing after the penultimate stage to reattach at entry to the following fixed blade row. As shown in Figs. 10 and 11, the curvature of the free streamline boundary thus formed can result in near radial flows at inlet to the final stage.

The measured yaw angles confirm that the leakage flow is deflected relatively little by the moving blades and therefore reaches the final stage with significant residual swirl. In turbine *B*, as described previously, the fixed blades are highly twisted and the incidence angle of the leakage flow is small. For the more orthodox design of turbine *A*, the leakage jet enters the final stage at high negative incidence, the consequent aerodynamic loss offsetting the 'carry-over' of kinetic energy. It can be seen, therefore, that it is important to include the appropriate distribution of flow rate and loss over the tip region in calculations of flow in L.P. cylinders. The practice of "applying" local efficiencies of 0.90 and 0.97 to the last two streamlines "at root and tip" as suggested by Forster *et al.* [5] would not be an accurate representation of, for example, turbine *B*.

6. Conclusions

The leakage flow from the penultimate stage is a particularly important feature of the flow in the final stage of large L.P. turbines. Its influence can be considerably more than a simple carryover of kinetic energy. The parallel sections of conventional turbine casings at the tip of the penultimate stage moving blades result in flow separation, the leakage jet forming the outer flow boundary. This boundary can deviate significantly from the actual casing surface and must be represented appropriately in axisymmetric turbine design calculations. In addition, the incidence of the leakage flow on the final stage fixed blades can introduce high losses which must also be included in any detailed analysis.

It has also been shown that aerodynamic losses in L.P. steam turbines can differ considerably in practice from commonly used design data. The "traditional" secondary flow vortices were not detected in the two machines tested, but profile losses were found to be approximately twice the values predicted by a widely used correlation method, possibly as a result of the presence of water.

Finally it has been shown that detailed measurements in operating turbines can provide valuable information on previously unknown aspects of the flow structure. With the introduction of increasingly sophisticated design methods, such measurements are considered essential in improving both the design procedures and the input data used.

Acknowledgements. The work was carried out at the Central Electricity Research Laboratories and the paper is published by permission of the Central Electricity Generating Board.

The authors would like to acknowledge the skill of Mr P. C. Skingley in constructing the probes, and of the assistance of Mr R. W. Langford with the turbine measurements.

Appendix I

The Setting of the Probe Head Axis Relative to the Traversing Arm and the Change of Flow Incidence During a Traverse

Fig. 15 shows a general velocity vector C of the flow in a turbine cylinder relative to cylindrical polar coordinates. The projection of this vector in the radial tangential plane is shown in Fig. 16 with the traverse arm and the probe head axis included. The angles between the probes head axis and the traverse arm in and normal to the radial tangential plane are Λ and δ respectively.

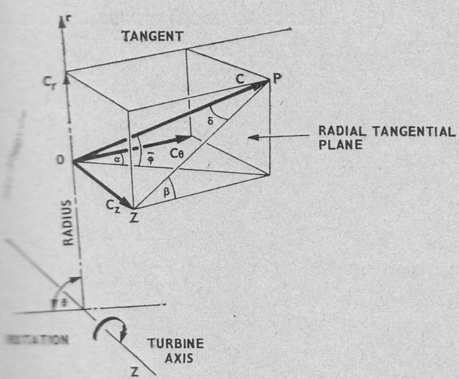

Fig. 15. Velocity components and flow angles

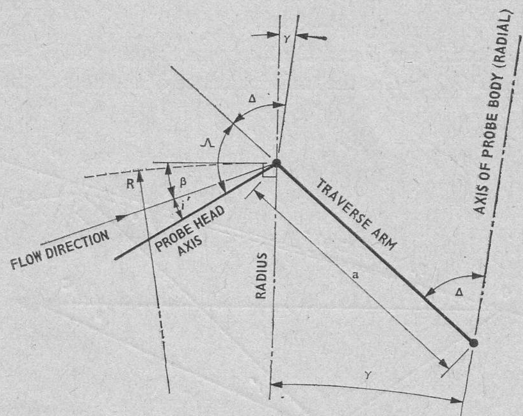

Fig. 16. General position of traverse arm projection in rad-tan plane

The incidence of the flow to the probe head axis in the rad-tan plane is from Fig. 16.

$$i' = \Lambda + \Delta - \left(\frac{\pi}{2} + \gamma + \beta\right), \tag{1}$$

where

$$\beta = \tan^{-1}\left(\frac{\tan\bar{\phi}}{\cos\delta}\right) \tag{2}$$

is the pitch angle in the rad-tan plane and

$$\gamma = \sin^{-1}\left(\frac{a}{R}\sin\Delta\right). \tag{3}$$

The probe head was set to align with the flow at mid traverse (denoted by subscript m), that is $i'=0$ giving setting angles
from (1)

$$\Lambda=\frac{\pi}{2}+\gamma_m+\beta-\Delta_m \tag{4}$$

and from Fig. 15

$$\delta=\sin^{-1}(\sin\alpha\cos\bar{\phi}). \tag{5}$$

For a typical configuration at exit from the fixed blades

Radius $R=1.7$m

Yaw angle $\alpha=18°$

Pitch angle $\bar{\phi}=16°$

The probe dimensions are $\Delta_m=31°$ and the length of the arm $a=0.33$m. Substitution in (1) and (5) gives

$\Lambda=82°$ and $\delta=17.3°$.

Fig. 17 shows the total incidence of the flow to the probe head as two components i and j when the incidence in the rad-tan plane is i'. The angle j of the projection of the velocity OP onto the plane OZP (where OZ is parallel to the turbine axis and OP is the probe head axis) is

$$j=\tan^{-1}\left(\frac{\tan\delta}{\cos i}\right)-\delta. \tag{6}$$

Substituting for δ and the likely maximum value $i'=20°$ gives $j<1$. Hence to good approximation the angle POQ $(=i)$ is the total incidence of the flow to the probe.

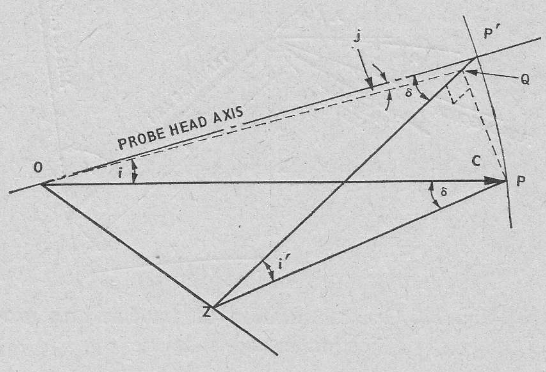

Fig. 17. Flow incidence components to the probe head axis

Substituting into (1) for Λ from (4) and for γ from (3) gives

$$i'=\Delta-\Delta_m+\sin^{-1}\left(\frac{a}{R}\sin\Delta_m\right)-\sin^{-1}\left(\frac{a}{R}\sin\Delta\right). \tag{7}$$

Hence i' is greatest at the largest value of Δ which from the probe dimensions will be $\Delta=50.3°$. Hence the maximum incidence in the rad-tan plane will be $i'=16.4°$. From Fig. 17

$$i=\sin^{-1}(\sin i'\cos\delta)$$

and therefore the incidence of the flow to the probe will not exceed $i=15.6°$.

Appendix II

The Calculation of Loss Coefficients

1. The calculation of the energy loss coefficient from traverse data

The energy loss coefficient from a blade row is defined as

$$\xi=\frac{\text{Isentropic downstream kinetic energy} - \text{Actual downstream kinetic energy}}{\text{Isentropic downstream kinetic energy}}.$$

When the static pressure has become circumferentially uniform downstream from the trailing edge ξ is given to a very good approximation by

$$\xi=\frac{2\delta}{p\sin\alpha}, \tag{8}$$

where p is the blade pitch, α the outlet flow angle (=yaw angle see Fig. 15) and δ_2 is the momentum thickness of the downstream wake. The value $\delta_2/\sin\alpha$ is, in effect, the momentum thickness of the circumferential distribution of axial velocity and is given by

$$\delta_{2s}=\delta_2/\sin\alpha=\int\limits_0 \frac{\rho U\sin\alpha\cos\bar{\phi}}{\rho_m U_m\sin\alpha_m\cos\bar{\phi}_m}\left(1-\frac{\rho U\sin\alpha\cos\bar{\phi}}{\rho_m U_m\sin\alpha_m\cos\bar{\phi}_m}\right)ds\,, \tag{9}$$

where the subscript m implies mid passage values corresponding to the maximum velocity at that radius.

It can be shown from the measured wake velocity variation that ρ/ρ_m is generally less than 0.99 for circumferentially uniform static pressure. Also if strong passage vortices are absent the circumferential variation in α and $\bar{\phi}$ will be small giving from (8) and (9).

$$\xi=\frac{2\delta_{2s}}{p}=\frac{2}{p}\int\limits_0^p \frac{U}{U_m}\left(1-\frac{U}{U_m}\right)ds\,. \tag{10}$$

2. Dunhams secondary loss correlation

Secondary loss coefficient

$$Y_s=\frac{\text{Stagnation pressure loss}}{\text{Downstream dynamic head}}.$$

Dunham [10] suggests

$$Y_s=\frac{c}{h}\frac{Z\cos\alpha_2}{\cos\beta_1}\left(0.0055+0.078\sqrt{\frac{\delta_1}{c}}\right), \tag{11}$$

where Z is Ainleys loading parameter

$$Z=\left(\frac{C_L}{s/c}\right)^2\frac{\cos^2\alpha_2}{\cos^2\alpha_m} \tag{12}$$

and C_L is the lift coefficient referred to the vector mean velocity

$$C_L=2s/c(\tan\alpha_1-\tan\alpha_2)\cos\alpha_m\,. \tag{13}$$

In Dunhams notation

c – chord, s – pitch, h – annulus height,

α_1 – flow inlet angle relative to blade,

α_2 – flow outlet angle relative to blade,

β_1 – blade inlet angle,

α_m – vector mean flow angle$=\tan^{-1}(\frac{1}{2}(\tan\alpha_1+\tan\alpha_2))$,

δ_1 – boundary layer displacement thickness.

The term $(0.0055+.078\ \delta_1/c)$ is a "tentative simple" formula suggested by Dunham as the function of the inlet wall boundary layer thickness. The function suggested more recently by Came [6] was not applied to the results of this investigation as the required axial flow velocity distribution at inlet could not be specified in the separated region.

3. The radial distribution of secondary loss

Y_s from Dunhams correlation gives the secondary loss of a cascade based on mid passage height conditions. To obtain an approximate radial distribution this is first expressed in energy loss terms using Whybrow's [16] relationship. The approximate radial distribution of secondary loss was than determined by assuming the components at root and tip were equal and equating

$$\dot{m}(\xi_s U_2^2)_{\text{MID PASSAGE}}=2(\rho U_{\text{axial}} 2\pi R z \xi_{\text{ST}} U_2^2)_{\text{TIP}}, \tag{13}$$

where values relating to the tip were taken as the mean over the estimated radial extent of the secondary loss region z. ξ_{ST} is the local value of secondary loss coefficient and $\dot{m}$ is the total mass flow at exit from the fixed blades. Values of z were taken from Came [6] depending on the incidence of the flow at inlet.

References

[1] R. A. Novak, *Streamline Curvature Computing Procedures for Fluid Flow Problems*. Tans. ASME Series A, vol. 89, 1967.

[2] L. H. Smith Jr., *The Radial Equilibrium Equation of Turbomachinery*. Trans. ASME Series A, vol. 88, 1966.

[3] W. Gracey, D. E. Coletti, and W. R. Russel, N. A. C. A. TN 2261, 1951.

[4] W. M. Schulze, G. C. Ashby, Jr., and J. R. Erwin, *Several Combination Probes for Surveying Static and Total Pressure and Flow Direction*. N.A.C.A. TN 2830, 1952.

[5] M. J. Moore, P. T. Walters, R. I. Crane, and B. J. Davidson, *Predicting the Fog-Drop Size in Wet-Steam Turbines*. I. Mech. E. Conference Publication 3, London 1973.

[6] P. M. Came, *Secondary Loss Measurements in a Cascade of Turbine Blades*. I. Mech. E. Conference Publication 3, London 1973.

[7] J. R. Turner, *An Investigation of the End-Wall Boundary Layer of a Turbine-Nozzle Cascade*. Trans. A.S.M.E. vol. 79, p. 1801, 1957.

[8] H. E. Rohlik, M. G. Kofskey, H. W. Allen, and H. A. Herzig, *Secondary Flows and Boundary Layer Accumulations in Turbine Nozzles*. N.A.C.A. Rep. 1168, 1954.

[9] W. G. Green, *Theory of Machines*, p. 221. Blackie and Son Ltd, London 1962.

[10] J. Dunham, *A Review of Cascade Data on Secondary Losses*. J. Mech. Enging. Sci. 1970 vol. 12 48.

[11] A. Klein, *Investigation of the Entry Boundary Layer on the Secondary Flows in the Blading of Axial Flow Turbines*. The British Hydromechanics Research Association Trans. 1004, 1969.

[12] O. E. Balje and R. I. Binsley, *Axial Turbine Performance Evaluation*. J. Engng. Pwr. Trans. A.S.M.E. 1968 (October).

[13] J. D. Denton, *A Survey and Comparison of Methods for Predicting the Profile Loss of Turbine Blades*. I. Mech. E. Conference Publication 3, London 1973.

[14] J. L. Kerrebrock and A. A. Mikolajczack, *Intra-Stator Transport of Rotor Wakes and Its Effect on Compressor Performance*. Trans. A.S.M.E. Series 'A' vol. 92, 1970.
[15] V. T. Forster, B. V. Archer, and R. G. Unsworth, *Experimental Facilities for Testing Scaled Models in Air or Freon*. I. Mech. E. Conference Publications 3, London 1973.
[16] J. F. T. Whybrow, *A Method of Estimating Axial Turbine Blading Performance*. Unpublished report of the C.E.G.B.
[17] I. I. Kirillov, and R. M. Yablonik, *Fundamentals of the Theory of Turbines Operating on Wet Steam*. NASA TT F-611.

Pomiary przepływu na obwodzie w ostatnich stopniach turbin niskoprężnych

Streszczenie

Opisano przyrząd służący do badań ciśnienia całkowitego w pobliżu ścianki zewnętrznej kadłuba w obszarze ostatnich stopni turbin niskoprężnych. Dzięki specjalnie zaprojektowanemu mechanizmowi łączników napędzającemu ramię, uzyskano możliwość przesuwania sondy Kiela w przepływie wzdłuż obwodu kadłuba. Ciśnienie całkowite na obwodzie mierzono co najmniej dla jednego odstępu łopatek.

Przedstawiono wyniki pomiarów przeprowadzonych w płaszczyźnie wylotu ostatniego stopnia dwu turbin o mocy 500 MW o różnej konstrukcji. W obu przypadkach wyniki pomiarów wskazują na istnienie prostej struktury śladów aerodynamicznych z bardzo nieznacznymi objawami przepływu wtórnego.

Zmiany ciśnienia statycznego dla istniejącego tu na obwodzie pola przepływu poddźwiękowego są pomijalne. Pola prędkości w tym obszarze można obliczyć z dobrym przybliżeniem na podstawie pomiarów ciśnienia statycznego wzdłuż promienia. To z kolei daje pogląd na rozkład współczynnika strat energii w kierunku promieniowym. Porównanie przewidywań teoretycznych z doświadczeniem wskazało na istnienie rozbieżności; problem ten przedyskutowano dla konkretnych geometrii kadłubów, których te badania dotyczyły. Przedstawione wyniki mają również znaczenie dla badań erozji łopatek i winny przyczynić się do poprawy metod projektowania turbin niskoprężnych.

Измерения течения на обводе последних ступеней турбин НД

Резюме

Описан прибор для исследования полного давления вблизи внешней стенки корпуса в районе последних ступеней турбин НД. Благодаря специально запроектированному механизму соединяющих элементов, приводящему рычаг, возникла возможность перемещения зонда Кила по обводу корпуса.

Полное давление замерялось на обводе не реже, чем один раз на шаг облопачивания.

Представлены результаты замеров, проведенных в плоскости выхода последней ступени двух турбин мощностью 500 Мвт различной конструкции. В обоих случаях результаты замеров указывают на простую структуру аэродинамических следов с очень незначительными симптомами вторичного течения.

Изменениями статического давления для происходящего на обводе дозвукового течения можно пренебрегать. Поля скоростей в этом районе можно рассчитать с хорошей точностью на основе замеров статического давления вдоль радиуса. Это дает представление о распределении коэффициента потерь энергии вдоль радиуса. Сравнение теоретических предпосылок с результатами эксперимента указывает на расхождение. Эта проблема дискутировалась для конкретных геометрических форм корпусов, которых эти исследования касались. Представленные результаты имеют большое значение для исследования эрозии лопаток и должны причиниться к усовершенствованию методов проектирования турбин НД.